Investigations of nonlinear induction motor model using the Gudermannian neural networks

Zulqurnain Sabir[1], Muhammad Asif Zahoor Raja[2], Dumitru Baleanu[3,4,d], R. Sadat[5], Mohamed R. Ali[6*]

[1]Department of Mathematics and Statistics, Hazara University, Mansehra, Pakistan
Email: zulqarnain_maths@hu.edu.pk

[2]Future Technology Research Center, National Yunlin University of Science and Technology, 123 University Road, Section 3, Douliou, Yunlin 64002, Taiwan, R.O.C.
Email: rajemaz@yuntech.edu.tw
[3]Department of Mathematics, Cankaya University, Ankara, Turkey
[4]Institute of Space Science, Magurele-Bucharest, Romania
dEmail: dumitrue@cankaya.edu.tr
[5]Department of Mathematics, Zagazig Faculty of Engineering, Zagazig University, Egypt

Email: r.mosa@zu.edu.eg

[6]Department of Basic Science, Faculty of Engineering at Benha, Benha University, 13512, Egypt

Email: mohamed.reda@bhit.bu.edu.eg

Abstract: This study aims to solve the nonlinear fifth-order induction motor model (FO-IMM) using the Gudermannian neural networks (GNNs) along with the optimization procedures of global search as a genetic algorithm together with the quick local search process as active-set technique (GNN-GA-AST). GNNs are executed to discretize the nonlinear FO-IMM to prompt the fitness function in the procedure of mean square error. The exactness of the GNN-GA-AST is observed by comparing the obtained results with the reference results. The numerical performances of the stochastic GNN-GA-AST are provided to tackle three different variants based on the nonlinear FO-IMM to authenticate the consistency, significance and efficacy of the designed stochastic GNN-GA-AST. Additionally, statistical illustrations are available to authenticate the precision, accuracy and convergence of the designed stochastic GNN-GA-AST.

Keywords: Gudermannain neural network; Fifth-order nonlinear induction motor model; Genetic algorithm; Statistical measures; Active-set technique.

1. Introduction

The induction motor nonlinear model together with two rotors circuits is indicated by a fifth-order of the differential system. The nonlinear fifth-order induction motor model (FO-IMM) is dependent upon two variables, one is the shaft speed and the second is the rotor state. In general, the two more variables are added using the second rotor circuit effects, which validate deep bars, starting cage and rotor distributed limits. To avoid the supplementary state of computational load variables with the mandatory routes of the additional rotor, the system is normally limited to the FO and rotor resistance is algebraically shifting as a rotor promptness function. This occurred due to the possibility when the frequency of rotor current depends on the speed of the rotor. This technique is operative for the steady-state response along with the sinusoidal energy [1].

The FO differential systems have been studied in the viscoelastic fluid systems [2-3]. Caglar et al. [4] implemented a sixth-degree B-spline to solve the linear/non-linear FO boundary value problems (BVPs). Agarwal studied the uniqueness and existence conditions of the results of such systems [5]. Noor et al [6] implemented a decomposition method to find the solutions of the FO-BVPs using the convergent series. Siddiqi et al [7–8] investigated the results of 6^{th}, 10^{th}, 12^{th} and 8^{th} order BVPs using the 6^{th}, 8^{th}, 10^{th} and 12^{th} spline degree, respectively. Siddiqi et al solved the special form of FO-BVPs using the non-polynomial spline and sextic methods [9-10]. Viswanadham et al. [11] solved a collocation method with B-splines of sixth order in terms of basis function to solve the special case of FO-BVPs. Akram et al [12] executed reproducing kernel space scheme to find the approximate solutions to FO-BVPs. Sabir et al [13] investigated the singular FO-BVPs using the variational iteration scheme. Viswanadham et al [14] provided a finite element approach, including the collocation method and quartic B-splines. Siddiqi et al. [15] implemented the non-polynomial spline approach to solve the singularly perturbed FO-BVPs. The generic form of the nonlinear FO-IMM is shown as [16]:

$$\begin{cases} u^{(5)}(\Psi) + f(\Psi)u(\Psi) = v(\Psi), & \Psi \in [p,q] \\ u(p) = c_0,\ u'(p) = c_1, u''(p) = c_2, & \\ u(q) = d_0,\ u'(q) = d_1. & \end{cases} \quad \textbf{(1)}$$

Where c_0, c_1, c_2, d_0 and d_1 are the real and finite constants, $f(\Psi)$ and $u(\Psi)$ are continuous on $[p,q]$. The above-stated schemes for the higher-order BVPs have their precise accuracy, capability and performance, as well as, confines over one another. However, the stochastic numerical solvers instigated by the Gudermannian neural networks (GNNs) along with the optimization procedures of global search as genetic algorithm together with the quick local search process as an active-set technique (GNN-GA-AST). The designed measures of GNN-GA-AST have never been implemented nor applied to solve the nonlinear FO-IMM. Few current proposals of the stochastic solvers are doubly singular models [17], biological prey-predator network [18], mosquito release system [19], singular Thomas-Fermi system [20], a nonlinear functional form of the singular systems [21-22], COVID-19 SITR system [23], SIR nonlinear dengue fever model [24], three-point differential model [25], heat conduction model [26], periodic boundary value singular problems [27] and infection HIV model [28]. The motive of the current work is to solve numerically the nonlinear FO-IMM using the stochastic procedures of GNN-GA-AST. Few novel characteristics of the GNN-GA-AST are briefly provided as:

- The design of GNN is accessible successfully to calculate the numerical outcomes of the nonlinear FO-IMM using the computing legacy of GA-AST.
- A consistent, consistent and precise overlapping of the outcomes is obtained by the stochastic procedures of GNN-GA-AST and the Adams results for solving the nonlinear FO-IMM.
- Certification of the stochastic GNN-GA-AST through the performance procedures based on the Theil's inequality coefficient (T.I.C), mean absolute deviation (MAD) and variance account for (VAF).
- The advantages and merits of the stochastic GNN-GA-AST are to accomplish a comprehensive framework for the nonlinear FO-IMM and to handle capably such nonlinear, stiff nature and complex higher-order models.

The remaining sections are organized as. Sec 2 shows the GNN-GA-AST methodology. Sec 3 provides the performance of statistical indices. Sec 4 shows the detailed discussions of the results, whereas, the concluding notes and reports based on future research are provided in the last Sec.

2. Methodology: GNN-GA-AST

This section is related to the design of the GNN-GA-AST to find the numerical measures of the nonlinear FO-IMM along with the fitness construction and the optimization procedures of GA-AST.

2.1 Construction of GNN

The procedures based on neural networks are prominent to find reliable, consistent and stable solutions in various fields. The mathematical representations of the nonlinear FO-IMM given in Eq (1) is stated with feed-forward neural networks in the form of approximate results together with their derivatives are written as:

$$\hat{u} = \sum_{l=1}^{k} m_l T(w_l \Psi + b_l), \tag{2}$$

$$\hat{u}^{(n)} = \sum_{l=1}^{k} m_l T^{(n)}(w_l \Psi + b_l), \tag{3}$$

In the above Eqs m_l, w_l and b_l shows the l^{th} components of the $\boldsymbol{m}$, $\boldsymbol{w}$ and $\boldsymbol{b}$ vectors, respectively, while $\hat{u}$ shows the form of approximate solutions. The Gudermannian activation function (GAF) i.e., $T(\Psi) = 2\tan^{-1}\left[\exp(\Psi)\right] - \frac{1}{2}\pi$ together with its FO derivative is used as an activation function. The updated form of the above system using the GAF is given as:

$$\hat{u}(\Psi) = \sum_{l=1}^{k} m_l \left(2\tan^{-1} e^{(w_l \Psi + b_l)} - \frac{\pi}{2} \right),$$

$$\hat{u}' = \sum_{l=1}^{k} 2 m_l w_l \left(\frac{e^{(w_l \Psi + b_l)}}{1 + \left(e^{(w_l \Psi + b_l)} \right)^2} \right),$$

$$\hat{u}'' = \sum_{l=1}^{k} 2 m_l w_l^{\,2} \left(\frac{e^{(w_l \Psi + b_l)}}{1 + e^{(2w_l \Psi + 2b_l)}} - \frac{2e^{(3w_l \Psi + 3b_l)}}{\left(1 + e^{(2w_l \Psi + 2b_l)}\right)^2} \right). \tag{4}$$

$$\hat{u}''' = \sum_{l=1}^{k} 2 m_l w_l^{\,3} \left(\frac{e^{(w_l \Psi + b_l)}}{1 + e^{(2w_l \Psi + 2b_l)}} - \frac{8e^{(3w_l \Psi + 3b_l)}}{\left(1 + e^{(2w_l \Psi + 2b_l)}\right)^2} + \frac{8e^{(5w_l \Psi + 5b_l)}}{\left(1 + e^{(2w_l \Psi + 2b_l)}\right)^3} \right)$$

$$\hat{u}^{(iv)} = \sum_{l=1}^{k} 2 m_l w_l^{\,4} \left(\frac{e^{(w_l \Psi + b_l)}}{1 + e^{(2w_l \Psi + 2b_l)}} - \frac{26e^{(3w_l \Psi + 3b_l)}}{\left(1 + e^{(2w_l \Psi + 2b_l)}\right)^2} + \frac{72e^{(5w_l \Psi + 5b_l)}}{\left(1 + e^{(2w_l \Psi + 2b_l)}\right)^3} - \frac{48e^{(7w_l \Psi + 7b_l)}}{\left(1 + e^{(2w_l \Psi + 2b_l)}\right)^4} \right)$$

The FO form of the derivative is written as:

$$\hat{u}^{(v)} = \sum_{l=1}^{k} 2m_l w_l^5 \left(\frac{e^{(w_l\Psi+b_l)}}{1+e^{(2w_l\Psi+2b_l)}} - \frac{80e^{(3w_l\Psi+3b_l)}}{\left(1+e^{(2w_l\Psi+2b_l)}\right)^2} + \frac{464e^{(5w_l\Psi+5b_l)}}{\left(1+e^{(2w_l\Psi+2b_l)}\right)^3} - \frac{768e^{(7w_l\Psi+7b_l)}}{\left(1+e^{(2w_l\Psi+2b_l)}\right)^4} + \frac{384e^{(9w_l\Psi+9b_l)}}{\left(1+e^{(2w_l\Psi+2b_l)}\right)^5} \right) \quad \textbf{(5)}$$

where the weight vector values are $\boldsymbol{m} = [m_1, m_2, m_3, ...m_l]$, $\boldsymbol{w} = [w_1, w_2, w_3, ..., w_l]$ and $\boldsymbol{b} = [b_1, b_2, b_3, ..., b_l]$, respectively. To solve the nonlinear FO-IMM, an error-based merit function is indicated as:

$$\Xi_{Fit} = \Xi_{Fit-I} + \Xi_{Fit-II}, \quad \textbf{(6)}$$

where Ξ_{Fit-1} and Ξ_{Fit-2} are the merit functions based on the mean square error sense, which is associated to the differential model and its BCs, respectively. An error function based on the nonlinear FO-IMM is given as:

$$\Xi_{Fit-I} = \frac{1}{N}\sum_{J=1}^{K}\left(\hat{u}_J^{(5)} + f_J v_J - \hat{u}_J)\right)^2,$$

$$\Xi_{Fit-2} = \frac{1}{5}\left(\left(\hat{u}_0 - c_0\right)^2 + \left(\hat{u}_0' - c_1\right)^2 + \left(\hat{u}_0'' - c_2\right)^2 + \left(\hat{u}_J - d_0\right)^2 + \left(\hat{u}_J' - d_1\right)^2\right).$$

2.2 Optimization process

The training of neural networks-based weight vectors is accomplished to function the computational strength procedure based on the GA-AST. The graphical representations of the stochastic procedures of GNN-GA-AST to solve the nonlinear FO-IMM are depicted in Fig. 1.

GA is known as an efficient global search process presented by Holand in the last century [29] and is operated to get the weight vectors (***W***) in neural networks modeling. The design of population with applicant explanations of GA is capable based on the values of real bounds. Though, each candidate result has some basics, which are equal to anonymous weights in the systems of neural networks. GA works over its dynamic operators as, elitism, crossover, mutation and selection. Recently, GA is implemented in recurrent optimization proposals like the heterogeneous bin storing [30], humanitarian logistics in emergency arrangement [31], lessen the cost in multi-energy building source [32], traveling salesman systems [33], design of residential buildings for building envelope [34], optimum set of identical clusters [35], glass transitions [36], Queen's problems [37] and prediction differential models [38].

The slowness of GA is reduced by using the process of hybridization with the appropriate local search approach by taking GA best values as an initial input. Subsequently, a well-ordered local search AST is implemented to adjust the parameters. AST is implemented in many recent applications, e.g., American better pricing choice on two assets [39], optimization with polyhedral constraints [40], pressure-dependent systems of water circulation based flow controls [41], numerical performances of the optimal control systems governed by the partial differential model [42], general constraints of the quadratic semidefinite program [43] and electrodynamic frictional contact models [44]. The detail of the implementation procedures of GA-AST is provided in the pseudocode-based Table 1.

Table 1: Pseudocode based on the optimization procedures using GA-ASA to solve the nonlinear FO-IMM

GA process starts

Inputs:

The constraints with the same number of system's elements as

$\boldsymbol{W}=[\boldsymbol{m},\mathbf{w},\mathbf{b}]$, where $\mathbf{m}=[m_1,m_2,m_3,...m_k]$, $\boldsymbol{w}=[w_1,w_2,...,w_p]$ and $\boldsymbol{S}=[b_1,b_2,b_3,...,b_k]$

Population: The chromosomes set is shown as: $\boldsymbol{P}=[\boldsymbol{W}_1,\boldsymbol{W}_2,...,\boldsymbol{W}_l]^t$.

Output: $\boldsymbol{W}_{\mathbf{GA-\ Best}}$ is the global Best weight value.

Initialization

Form $\boldsymbol{W}$ that shows the weights of real bounded numbers. The vectors set is to design a population $\boldsymbol{P}$. Normalize the [GA] generations.

Fitness (Ξ_{Fit}) structure

Attained Ξ_{Fit} in the population $\boldsymbol{P}$ for $\boldsymbol{W}$ based on Eq (7)

Termination Values

Procedure can terminate, if any condition is accomplished like as Ξ_{Fit} = 10^{-22}, Population Size =180, StallGenLimit=120

Generations=70, TolFun= TolCon =10^{-21}, Other values: default

Go to [**storage]**, to achieve the above-mentioned values.

Ranking

Well-organised dissimilar $\boldsymbol{W}$ in $\boldsymbol{P}$ population for Ξ_{Fit}.

Storage

Save $\boldsymbol{W}_{\mathbf{GA-\ Best}}$, generation, Ξ_{Fit}, time and count of function

GA Process Ends

Start of AST

Inputs

Inputs: $\boldsymbol{W}_{\mathbf{GA\text{-}Best}}$

Output

Best GA-AST weights are designated as $\boldsymbol{W}_{\mathbf{GA\text{-}AST}}$

Initialize

Assignments, iterations, Limited constraints and other specified values.

Terminate

The method stops to achieve any of the condition as:

$\Xi_{Fit} \leq 10^{-20}$, TolCon= TolFun=10^{-22}, Iterations = 510, TolX=10^{-21}

And MaxFunEvals=239000

While (Dismiss)

Assessment of Ξ_{Fit}

Compute Ξ_{Fit} of the weight vector values $\boldsymbol{W}$ for Eq (7).

Adaptations

Invoke {fmincon} in AST. Control $\boldsymbol{W}$ for each AST

generation. Calculate Ξ_{Fit} to shorten $\boldsymbol{W}$ for Eq 7

Store

Store $\boldsymbol{W}_{\textbf{GA-AST}}$, Ξ_{Fit}, count of function, time, iterations and AST current runs.

AST End

Data Generations

The process is repeated 30 times using the GA-AST to enhance a massive GNN dataset via the optimization variables to solve the nonlinear FO-IMM

3. Statistical measures

The performance soundings using different statistical performances based on the MAD, T.I.C and V.A.F to validate the constancy and reliability are provided for solving the nonlinear FO-IMM. The mathematical depictions of these operatives are written as:

$$\text{MAD}=\sum_{l=1}^{i}\left|u_l-\hat{u}_l\right| \tag{7}$$

$$\text{T.I.C}=\frac{\sqrt{\frac{1}{n}\sum_{l=1}^{i}\left(u_l-\hat{u}_l\right)^2}}{\left(\sqrt{\frac{1}{n}\sum_{l=1}^{i}u_l^2}+\sqrt{\frac{1}{n}\sum_{l=1}^{i}\hat{u}_l^2}\right)}, \tag{8}$$

$$\begin{cases}\text{V.A.F}=\left(1-\dfrac{\text{var}\left(u_l-\hat{u}_l\right)}{\text{var}\left(u_l\right)}\right)*100\\ \text{EVAF}=\left|100-\text{V.A.F}\right|.\end{cases} \tag{9}$$

4. Simulations of the Results

In this section, the detail of the numerical solutions to solve three dissimilar problems of the nonlinear FO-IMM are provided along with the illustrations of the suitable graphs and tables.

Problem I: Consider the nonlinear FO-IMM having trigonometric ratios

$$\begin{cases}u^{(5)}(\Psi)+\sin(\Psi)u(\Psi)=\sin(\Psi)\left(\sin(\Psi)-1\right)+\cos(\Psi)\left(\sin(\Psi)+1\right), \quad \Psi\in[0,1]\\ u(0)=1,\ u'(0)=1, u''(0)=-1,\\ u1)=\sin(1)+\cos(1),\ u'(1)=-\sin(1)+\cos(1).\end{cases} \tag{10}$$

The exact solution of the above nonlinear FO-IMM is $\sin(\Psi)+\cos(\Psi)$, whereas the Ξ_{Fit} is given as:

$$\Xi_{Fit}=\frac{1}{N}\sum_{l=1}^{I}\left(\hat{U}_{L}^{(5)}+\sin(\Psi_{L})\hat{u}_{l}-\sin(\Psi_{l})\left(\sin(\Psi_{l})-1\right)-\cos(\Psi_{l})\left(\sin(\Psi_{l})+1\right)\right)^{2}$$
$$+\frac{1}{5}\left(\begin{array}{l}\left(\hat{u}_{0}-1\right)^{2}+\left(\hat{u}_{0}'-1\right)^{2}+\left(\hat{u}_{0}''+1\right)^{2}\\+\left(\hat{u}_{I}-\sin(1)-\cos(1)\right)^{2}+\left(\hat{u}_{I}'+\sin(1)-\cos(1)\right)^{2}\end{array}\right). \quad \textbf{(11)}$$

Problem II: Consider a nonlinear FO-IMM having trigonometric ratios and exponential functions are given as:

$$\begin{cases}u^{(5)}(\Psi)+u(\Psi)=4e^{\Psi}\cos(\Psi)-2e^{\Psi}\left(\sin(\Psi)-1\right)+5e^{\Psi}\sin(\Psi), & \Psi\in[0,1]\\ u(0)=1,\ u'(0)=0,u''(0)=-1,\\ u(1)=-e\left(\sin(1)-1\right),\ u'(1)=e-e\left(\sin(1)+\cos(1)\right).\end{cases} \quad \textbf{(12)}$$

The exact solution of the above nonlinear FO-IMM is $-e^{\Psi}\left(\sin(\Psi)-1\right)$, whereas the Ξ_{Fit} is given as:

$$\Xi_{Fit}=\frac{1}{N}\sum_{l=1}^{I}\left(\hat{u}_{l}^{(5)}+\hat{u}_{l}-4e^{\Psi_{l}}\cos(\Psi_{l})+2e^{\Psi_{l}}\left(\sin(\Psi_{l})-1\right)-5e^{\Psi_{l}}\sin(\Psi_{l})\right)^{2}$$
$$+\frac{1}{5}\left(\begin{array}{l}\left(\hat{u}_{0}-1\right)^{2}+\left(\hat{u}_{0}'\right)^{2}+\left(\hat{u}_{0}''+1\right)^{2}\\+\left(\hat{u}_{I}+\left(e\sin(1)-1\right)\right)^{2}+\left(\hat{u}_{I}'-e+e\left(\sin(1)+\cos(1)\right)\right)^{2}\end{array}\right). \quad \textbf{(13)}$$

Problem III: Consider a nonlinear FO-IMM having exponential terms is shown as:

$$\begin{cases}u^{(5)}(\Psi)-u(\Psi)=-e^{\Psi}\left(10\Psi+15\right), & \Psi\in[0,1]\\ u(0)=0,\ u'(0)=1,u''(0)=0,\\ u(1)=0,\ u'(1)=-e.\end{cases} \quad \textbf{(14)}$$

The exact solution of the above nonlinear FO-IMM is $-\Psi e^{\Psi}\left(\Psi-1\right)$, whereas the Ξ_{Fit} is given as:

$$\Xi_{Fit}=\frac{1}{N}\sum_{l=1}^{I}\left(\hat{u}_{l}^{(5)}-\hat{u}_{l}+e^{\Psi_{l}}\left(10(\Psi_{l})+15\right)\right)^{2}+\frac{1}{5}\left(\left(\hat{u}_{0}\right)^{2}+\left(\hat{u}_{0}'-1\right)^{2}+\left(\hat{u}_{0}''\right)^{2}+\left(\hat{u}_{I}\right)^{2}+\left(\hat{u}_{I}'+e\right)^{2}\right). \quad \textbf{(15)}$$

The obtained form of the GNN using the process of GA-AST optimization is implemented to solve three dissimilar problems of the nonlinear FO-IMM. The performances of the best weights are authenticated to attain the numerical procedures of the nonlinear FO-IMM. The mathematical notations of the unidentified weight vectors are given as:

$$\hat{u}_1(\Psi) = -0.047(2\tan^{-1}e^{(2.7437\Psi+3.5439)} - 0.5\pi) - 3.3677(2\tan^{-1}e^{(-0.010\Psi+5.5374)} - 0.5\pi)$$
$$-0.6601(2\tan^{-1}e^{(-0.1635\Psi-1.4745)} - 0.5\pi) - 3.5449(2\tan^{-1}e^{(0.6113\Psi-1.1695)} - 0.5\pi)$$
$$+2.8944(2\tan^{-1}e^{(-1.264\Psi+3.6520)} - 0.5\pi) - 0.2364(2\tan^{-1}e^{(-0.500\Psi-4.7829)} - 0.5\pi) \quad \textbf{(16)}$$
$$+2.5679(2\tan^{-1}e^{(1.3422\Psi-3.8539)} - 0.5\pi) - 1.3510(2\tan^{-1}e^{(-0.7714\Psi-0.5473)} - 0.5\pi)$$
$$-1.4685(2\tan^{-1}e^{(-0.679\Psi+0.0481)} - 0.5\pi) - 1.5016(2\tan^{-1}e^{(-0.2449\Psi-0.4754)} - 0.5\pi),$$

$$\hat{u}_2(\Psi) = 20.627(2\tan^{-1}e^{(1.1868\Psi+22.150)} - 0.5\pi) + 23.8505(2\tan^{-1}e^{(5.6419\Psi+6.3215)} - 0.5\pi)$$
$$+23.297(2\tan^{-1}e^{(29.323\Psi+29.549)} - 0.5\pi) + 11.3852(2\tan^{-1}e^{(23.057\Psi+28.993)} - 0.5\pi)$$
$$-19.061(2\tan^{-1}e^{(3.4279\Psi+3.0421)} - 0.5\pi) - 20.2783(2\tan^{-1}e^{(1.6518\Psi+2.3957)} - 0.5\pi) \quad \textbf{(17)}$$
$$-26.541(2\tan^{-1}e^{(-2.522\Psi+8.5805)} - 0.5\pi) - 26.1822(2\tan^{-1}e^{(-2.702\Psi-2.535)} - 0.5\pi)$$
$$+15.181(2\tan^{-1}e^{(-15.545\Psi-23.643)} - 0.5\pi) - 24.4045(2\tan^{-1}e^{(11.174\Psi+11.68)} - 0.5\pi),$$

$$\hat{u}_3(\Psi) = -6.960(2\tan^{-1}e^{(-1.299\Psi+26.75)} - 0.5\pi) + 17.408(2\tan^{-1}e^{(-0.190\Psi-0.4086)} - 0.5\pi)$$
$$-2.5188(2\tan^{-1}e^{(1.3239\Psi-2.6631)} - 0.5\pi) - 29.756(2\tan^{-1}e^{(2.1568\Psi-5.2853)} - 0.5\pi)$$
$$-4.5499(2\tan^{-1}e^{(-0.297\Psi+8.950)} - 0.5\pi) - 2.9270(2\tan^{-1}e^{(-0.519\Psi-0.9318)} - 0.5\pi) \quad \textbf{(18)}$$
$$-9.0905(2\tan^{-1}e^{(-0.663\Psi+0.948)} - 0.5\pi) + 5.7747(2\tan^{-1}e^{(-0.089\Psi-16.3950)} - 0.5\pi)$$
$$+2.6309(2\tan^{-1}e^{(2.4358\Psi-5.136)} - 0.5\pi) - 4.2711(2\tan^{-1}e^{(3.6500\Psi+15.5738)} - 0.5\pi),$$

The graphical presentations of the GNN-GA-AST are illustrated to solve all three problems of the nonlinear FO-IMM in Figs 1 to 4. The performance of the GNN-GA-AST using the optimization measures is implemented for thirty independent runs. Fig. 1 illustrates the weights vector plots using the Eqs 16 to 18 along with the outcome's comparisons based on best, mean and exact solutions of the nonlinear FO-IMM using the GNN-GA-AST. It is observed that the calculated results using GNN-GA-AST overlapped with mean and exact solutions for each problem of the nonlinear FO-IMM. The values of the AE are illustrated in Fig. 2(a) and one can observe that the best AE values lie around 10^{-06} to 10^{-08}, 10^{-03} to 10^{-05} and 10^{-04} to 10^{-05} for problems I, II and III of the nonlinear FO-IMM. Fig 2(b) represents the performance trials for problems I, II and III of the nonlinear FO-IMM. The performances of the best FIT found around 10^{-08} to 10^{-10}, 10^{-06} to 10^{-07} and 10^{-04}-10^{-05} for problems I, II and III. The best values of the MAD operator lie in the ranges of 10^{-06}-10^{-07}, 10^{-05}-10^{-06} and 10^{-03} to 10^{-04} for problems I, II and III. The best values of the T.I.C operator lie in the ranges of 10^{-09}-10^{-10}, 10^{-08}-10^{-09} and 10^{-06} to 10^{-07} for problems I, II and III. The best values of the EVAF operator lie in the ranges of 10^{-11}-10^{-12}, 10^{-09}-10^{-10} and 10^{-04} to 10^{-05} for problems I, II and III. It is proved the accuracy of the proposed GNN-GA-AST through these statistical soundings to solve the problems I, II and III of the nonlinear FO-IMM.

The graphical depictions of the statistical processes and histograms are plotted in Figs. 3 and 4 for the problems I, II and III of the nonlinear FO-IMM. The convergence plots of FIT, MAD,

T.I.C and E.VAF are derived for thirty runs based on the nonlinear FO-IMM. The obtained results demonstrated the suitable routines that are about 80% trials based on the FIT, E.VAF, T.I.C and MAD.

To get more satisfaction of the GNN-GA-AST, the performance of the statistical measures is investigated for thirty runs using mean, minimum (Min) and semi interquartile range (S.I.R) to solve the FO-IMM. The Min values indicate the best runs and the S.I.R is the $\frac{1}{2}(Q_3 - Q_1)$, where Q_1 and Q_3 are the 1st and 3rd quartiles. The statistical Mean, S.I.R and Min procedures are tabulated in Table 2 that validates very good performances to solve all problems of the FO-IMM. Table 3 shows the computational capability of the stochastic GNN-GA-AST based on the completed generations, timely execution and functions count to perceive the decision variables of the system.

Case 1

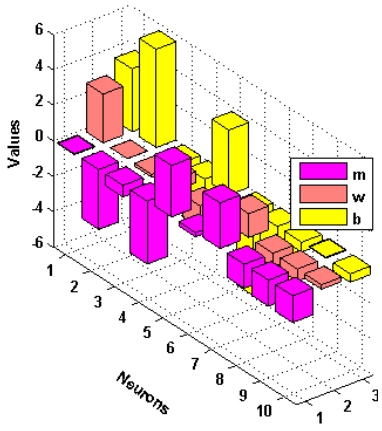

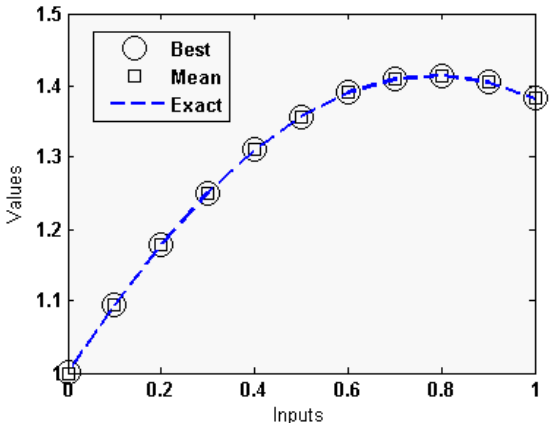

Case 2

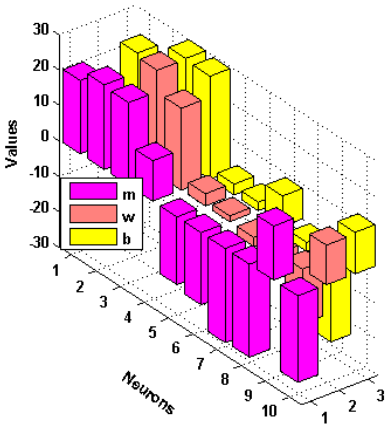

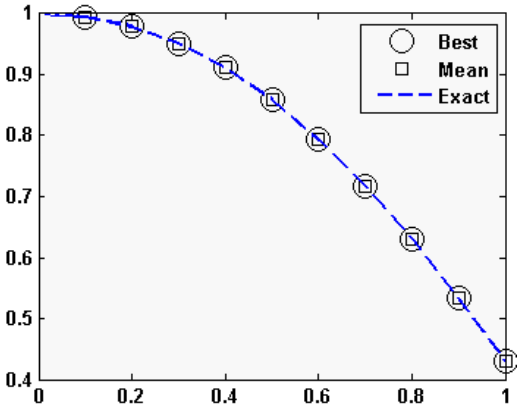

Case 3

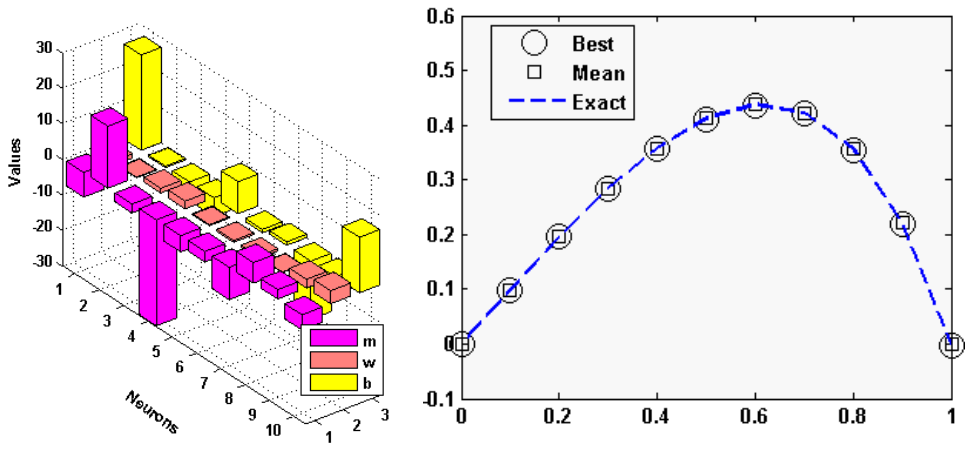

Figure 1: Best weights, comparison of best, exact and mean results to solve the FO-IMM

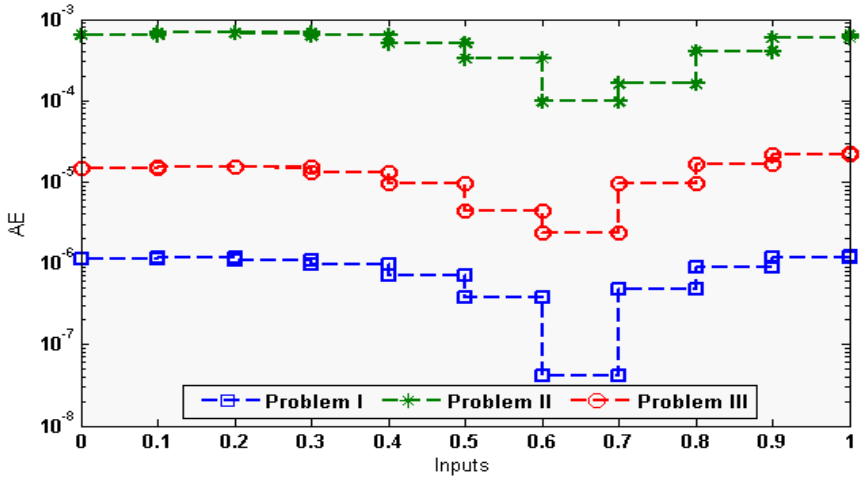

(a) AE values for problems I, II and III to solve the FO-IMM

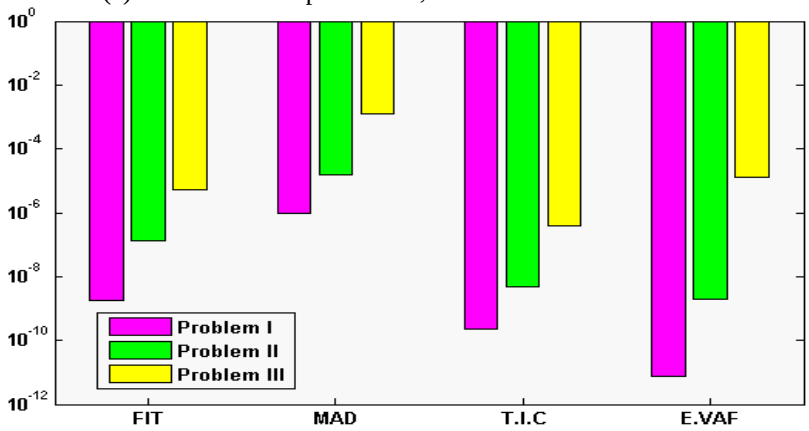

(b) Performance soundings for problems I, II and III to solve the FO-IMM

Figure 2: AE values and performance investigations based on FIT, MAD, T.I.C and E.VAF operators for problems I, II and III to solve the FO-IMM

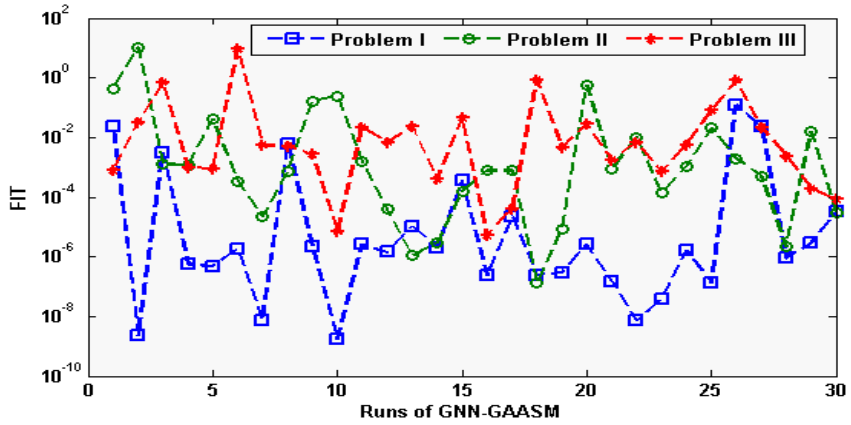

Performance of FIT values in convergence studies to solve FO-IMM

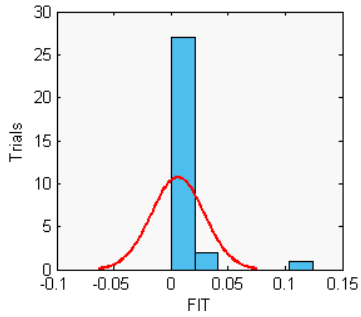

(a) Hist: Problem I

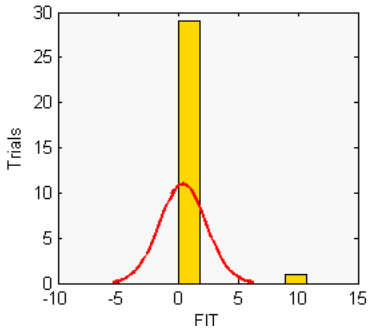

(b) Hist: Problem II

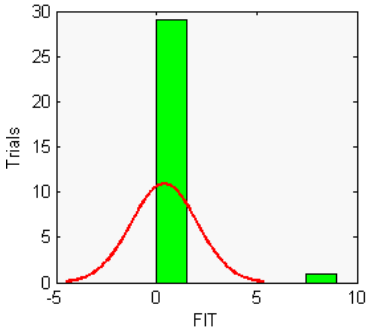

(c) Hist: Problem III

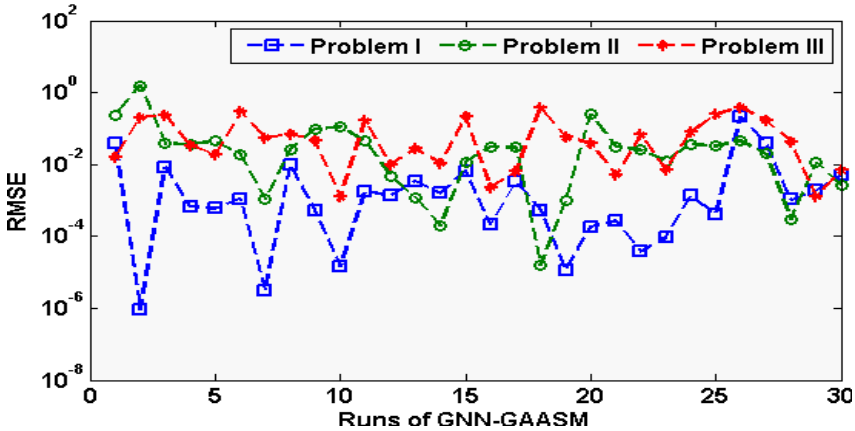

Performance of RMSE values in convergence studies to solve FO-IMM

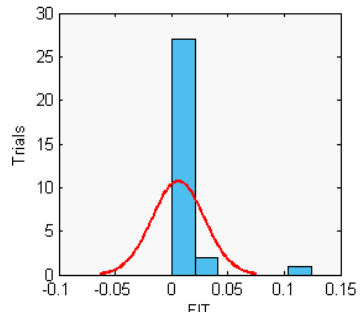

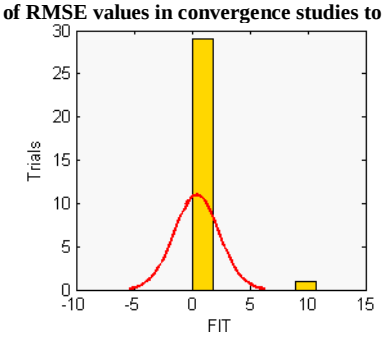

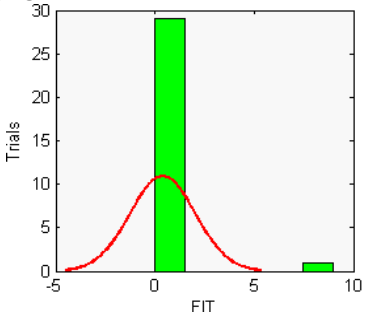

(d) Hist: Problem I **(e) Hist: Problem II** **(f) Hist: Problem III**

Figure 3: FIT and MAD Convergences plots along with Hist values using the optimization process of GA-AST to solve the FO-IMM

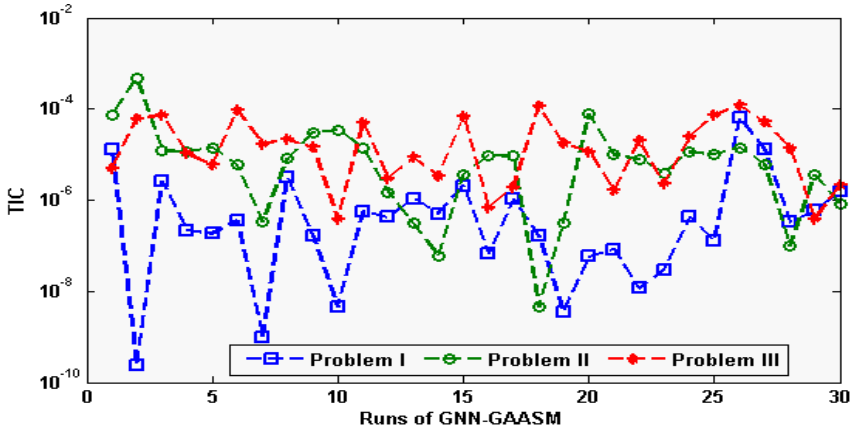

Performance of T.I.C values in convergence studies to solve FO-IMM

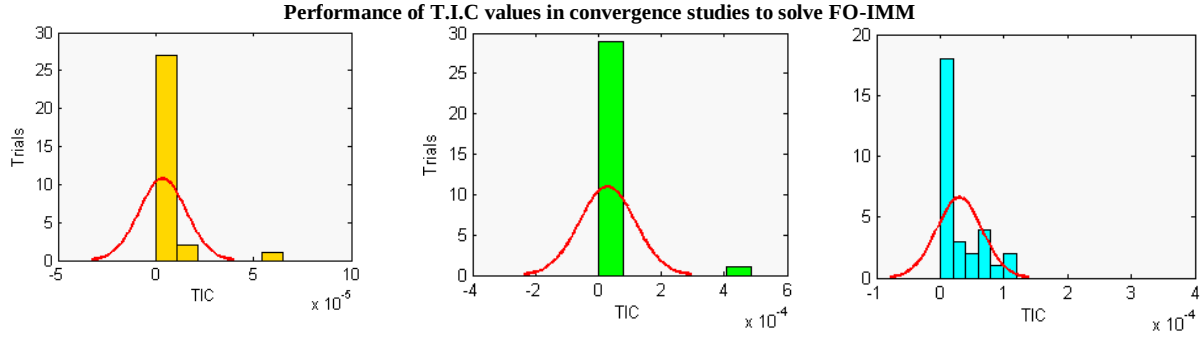

(a) Hist: Problem I **(b) Hist: Problem II** **(c) Hist: Problem III**

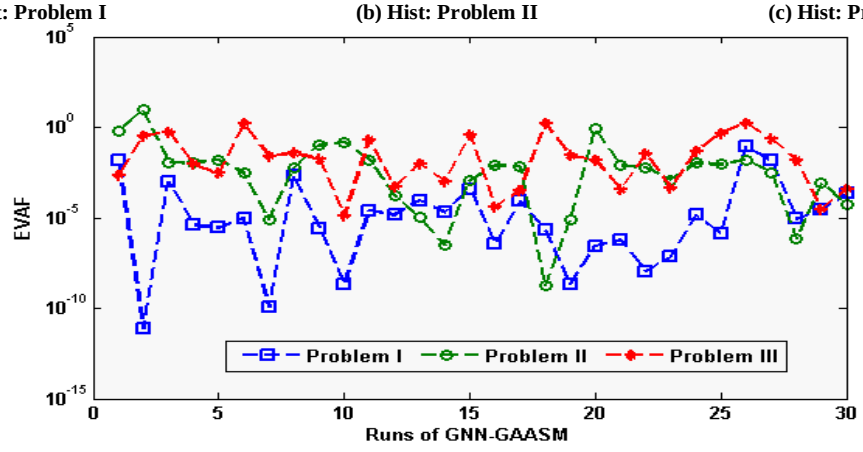

Performance of EVAF values in convergence studies to solve FO-IMM

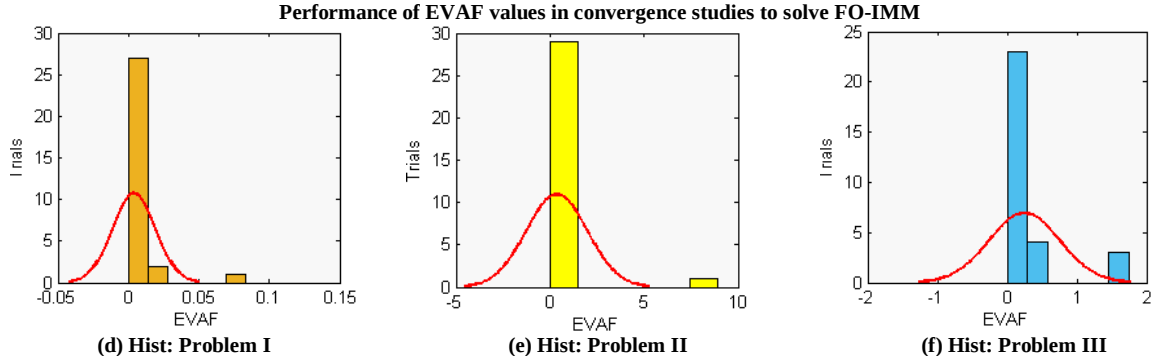

(d) Hist: Problem I **(e) Hist: Problem II** **(f) Hist: Problem III**

Figure 4: T.I.C and EVAF Convergences plots along with Hist values using the optimization process of GA-AST to solve the FO-IMM

Table 2: Statistics inquiries to solve each problem of the nonlinear FO-IMM

Ψ	Problem I			Problem II			Problem III		
	Min	**Mean**	**S.I.R**	**Min**	**Mean**	**S.I.R**	**Min**	**Mean**	**S.I.R**
0	1.148E-06	1.075E-03	1.770E-03	1.918E-05	3.390E-02	2.413E-02	1.832E-04	4.748E-02	9.449E-02
0.1	1.155E-06	1.397E-03	2.083E-03	2.024E-05	2.386E-02	2.192E-02	8.921E-05	5.830E-02	9.326E-02
0.2	1.105E-06	1.405E-03	1.100E-03	2.036E-05	2.471E-02	2.151E-02	8.745E-05	5.890E-02	9.989E-02
0.3	9.654E-07	1.044E-03	1.838E-03	1.886E-05	2.281E-02	1.996E-02	3.480E-04	5.396E-02	8.219E-02
0.4	7.204E-07	1.062E-03	1.599E-03	1.545E-05	2.761E-02	1.617E-02	6.799E-04	4.518E-02	3.421E-02
0.5	3.764E-07	6.915E-04	1.055E-03	1.014E-05	1.905E-02	1.594E-02	8.725E-04	3.055E-02	4.605E-02
0.6	4.071E-08	2.169E-04	3.564E-04	3.333E-06	5.438E-03	5.101E-03	3.227E-04	1.235E-02	1.746E-02
0.7	4.851E-07	3.024E-04	3.835E-04	4.234E-06	9.739E-03	1.695E-02	1.437E-04	1.699E-02	2.391E-02
0.8	7.851E-07	8.149E-04	1.162E-03	1.147E-05	2.306E-02	1.622E-02	8.042E-04	3.202E-02	5.927E-02
0.9	3.747E-07	1.195E-03	1.083E-03	1.694E-05	3.100E-02	2.170E-02	1.229E-03	4.813E-02	8.827E-02
1	2.688E-07	1.327E-03	2.037E-03	1.884E-05	2.380E-02	1.895E-02	1.377E-03	5.386E-02	9.750E-02

Table 3: Complexity measures to solve each problem of the nonlinear FO-IMM

Problem	**Generations**		**Implementation of time**		**Functions count**	
	Mean	**STD**	**Mean**	**STD**	**Mean**	**STD**
I	105.5662	8.0787	305.0000	21.2872	19570.5000	786.6982
II	104.7645	6.8842	305.0000	24.8973	19661.6667	584.8162
III	104.5080	5.4628	305.0000	20.8765	19579.9667	85.9155

4. Concluding remarks

The present investigations are related to solve the nonlinear FO-IMM by exploiting the GNNs together with the hybridization techniques of global and local search schemes, GNN-GA-AST. An error function using the differential system and its corresponding initial conditions is considered and then optimized using the computational process of GA-AST. The correctness and exactness of the stochastic GNN-GA-AST are pragmatic to compare the obtained results with the true solutions. The values of the AE are observed in good measures and found around 10^{-06} to 10^{-08} for solving the nonlinear FO-IMM. The performance of the GA-AST using different statistical measures is calculated to solve the nonlinear FO-IMM. To validate the stability, capability and reliability of the GNN-GA-AST, dissimilar statistical performances using the EVAF, MAD and T.I.C operatives have been available to find the precise and accurate results of the nonlinear FO-IMM. Moreover, the statistical measures for thirty independent trials are also measured and most of the trials showed the highest level of accuracy to solve the nonlinear FO-IMM.

In the future, the stochastic GNN-GA-AST can be used to solve the prediction models, fluid dynamic models and biological systems.

References

[1] Richards, G. et al., 1994. Reduced order models for induction motors with two rotor circuits. IEEE Transactions on Energy Conversion, 9(4), pp.673-678.

[2] Davies, A.R., et al., 1988. Spectral Galerkin methods for the primary two-point boundary value problem in modelling viscoelastic flows. *International Journal for Numerical Methods in Engineering*, *26*(3), pp.647-662.

[3] Karageorghis, A., et al., 1988. Spectral collocation methods for the primary two-point boundary value problem in modelling viscoelastic flows. International Journal for Numerical Methods in Engineering, 26(4), pp.805-813.

[4] Caglar, H.N., et al., 1999. The numerical solution of fifth-order boundary value problems with sixth-degree B-spline functions. Applied Mathematics Letters, 12(5), pp.25-30.

[5] Agarwal, R.P., 1986. Boundary value problems from higher order differential equations. World Scientific.

[6] Noor, M.A. et al., 2009. A new approach to fifth-order boundary value problems. International Journal of Nonlinear Science, 7(2), pp.143-148.

[7] Siddiqi, S.S., et al., 1996. 1. Spline Solutions of Linear Sixth-order Boundary-value Problems. Computer Methods in Applied Mechanics and Engineering, 31, pp.309-325.

[8] Siddiqi, S.S. et al., 1996. Spline solutions of linear sixth-order boundary-value problems. International Journal of Computer Mathematics, 60(3-4), pp.295-304.

[9] Siddiqi, S.S. et al., 2007. Sextic spline solutions of fifth order boundary value problems. Applied Mathematics Letters, 20(5), pp.591-597.

[10] Akram, G. et al 2017. Application of homotopy analysis method to the solution of ninth order boundary value problems in AFTI-F16 fighters. Journal of the Association of Arab Universities for Basic and Applied Sciences, 24, pp.149-155.

[11] Viswanadham, K.K., et al 2010. Numerical solution of fifth order boundary value problems by collocation method with sixth order B-splines. International Journal of Applied Science and Engineering, 8(2), pp.119-125.

[12] Akram, G. et al., 2011. Solution of fifth order boundary value problems in reproducing kernel space. Middle-East Journal of Scientific Research, 10(2), pp.191-195.

[13] Sabir, Z., et al, O., 2020. Numerical investigations to design a novel model based on the fifth order system of Emden–Fowler equations. Theoretical and Applied Mechanics Letters, 10(5), pp.333-342.

[14] NS KasiViswanadham, K. et al., 2012. Quartic B-spline collocation method for fifth order boundary value problems. International Journal of Computer Applications, 43(13), pp.1-6.

[15] Siddiqi, S.S., et al, A., 2011. Solution of fifth-order singularly perturbed boundary value problems using non-polynomial spline technique Euro. J Sci Res, 56, pp.415-425.

[16] Siddiqi, S.S. et al, M., 2015. Application of non-polynomial spline to the solution of fifth-order boundary value problems in induction motor. Journal of the Egyptian Mathematical Society, 23(1), pp.20-26.

[17] Raja, M.A.Z. et al., 2019. Numerical solution of doubly singular nonlinear systems using neural networks-based integrated intelligent computing. Neural Computing and Applications, 31(3), pp.793-812.

[18] Umar, M., 2019. Intelligent computing for numerical treatment of nonlinear prey–predator models. Applied Soft Computing, 80, pp.506-524.

[19] Umar, M. et al., 2020. A stochastic computational intelligent solver for numerical treatment of mosquito dispersal model in a heterogeneous environment. The European Physical Journal Plus, 135(7), pp.1-23.

[20] Sabir, Z. et al., 2018. Neuro-heuristics for nonlinear singular Thomas-Fermi systems. Applied Soft Computing, 65, pp.152-169.

[21] Sabir, Z. et al., 2019. Stochastic numerical approach for solving second order nonlinear singular functional differential equation. Applied Mathematics and Computation, 363, p.124605.

[22] Sabir, Z et al., 2020. Neuro-swarm intelligent computing to solve the second-order singular functional differential model. The European Physical Journal Plus, 135(6), p.474.

[23] Sabir, Z., Ali, M.R., Raja, M.A.Z. et al. Computational intelligence approach using Levenberg–Marquardt backpropagation neural networks to solve the fourth-order nonlinear system of Emden–Fowler model. Engineering with Computers (2021). https://doi.org/10.1007/s00366-021-01427-2.

[24] Ayub, A., Sabir, Z., Altamirano, G.C. et al. Characteristics of melting heat transport of blood with time-dependent cross-nanofluid model using Keller–Box and BVP4C method. Engineering with Computers (2021). https://doi.org/10.1007/s00366-021-01406-7.

[25] Sabir, Z. et al., 2020. Design of stochastic numerical solver for the solution of singular three-point second-order boundary value problems. Neural Computing and Applications, pp.1-17.

[26] Raja, M.A.Z., et al, 2018. A new stochastic computing paradigm for the dynamics of nonlinear singular heat conduction model of the human head. The European Physical Journal Plus, 133(9), p.364.

[27] Wen-Xiu Ma, Mohamed R. Ali, R. Sadat, "Analytical Solutions for Nonlinear Dispersive Physical Model", Complexity, vol. 2020, Article D 3714832, 8 pages, 2020. https://doi.org/10.1155/2020/3714832.

[28] Mohamed R. Ali , Dumitru Baleanu, New wavelet method for solving boundary value problems arising from an adiabatic tubular chemical reactor theory, International Journal of BiomathematicsVol. 13, No. 07, 2050059 (2020).

[29] Mohamed M. Mousa, Mohamed R. Ali & Wen-Xiu Ma, A combined method for simulating MHD convection in square cavities through localized heating by method of line and penalty-artificial compressibility, Journal of Taibah University for Science, 15:1, 208-217, (2021). DOI: 10.1080/16583655.2021.1951503..

[30] Sridhar, R.et al. "Optimization of heterogeneous Bin packing using adaptive genetic algorithm." In IOP Conference Series: Materials Science and Engineering, vol. 183, no. 1, p. 012026. IOP Publishing, 2017

[31] Chang, F. S., 2016. Greedy-Search-based Multi-Objective Genetic Algorithm for Emergency Humanitarian Logistics Scheduling.

[32] An, P. Q. et al., 2016, August. One-day-ahead cost optimisation for a multi-energy source building using a genetic algorithm. In Control (CONTROL), 2016 UKACC 11th International Conference on (pp. 1-6). IEEE.

[33] Vaishnav, P. et al., 2017. Traveling Salesman Problem Using Genetic Algorithm: A Survey.

[34] Tuhus-Dubrow, D. et al., 2010. Genetic-algorithm based approach to optimize building envelope design for residential buildings. Building and environment, 45(7), pp. 1574-1581.

[35] Das, S. et al., 2017, February. Optimal Set of Overlapping Clusters Using Multi-objective Genetic Algorithm. In Proceedings of the ninth International Conference on Machine Learning and computing (pp. 232-237). ACM.

[36] Tan, J. et al., 2017. Determination of glass transitions in boiled candies by capacitance based thermal analysis (CTA) and genetic algorithm (GA). Journal of Food Engineering, 193, pp. 68-75.

[37] Alharbi, S.et al., 2017. A genetic algorithm based approach for solving the minimum dominating set of queens problem. Journal of Optimization, 2017.

[38] Sabir, Z. et al., 2020. Integrated neuro-evolution heuristic with sequential quadratic programming for second-order prediction differential models. Numerical Methods for Partial Differential Equations.

[39] Gao, Y., et al., 2020. Primal-dual active set method for pricing American better-of option on two assets. Communications in Nonlinear Science and Numerical Simulation, 80, p.104976.

[40] Hager, W.W. et al., 2020. A Newton-type Active Set Method for Nonlinear Optimization with Polyhedral Constraints. arXiv preprint arXiv:2011.01201.

[41] Piller, O., et al., 2020. A Content-Based Active-Set Method for Pressure-Dependent Models of Water Distribution Systems with Flow Controls. Journal of Water Resources Planning and Management, 146(4), p.04020009.

[42] Azizi, M., et al., 2020. A fuzzy system based active set algorithm for the numerical solution of the optimal control problem governed by partial differential equation. European Journal of Control, 54, pp.99-110.

[43] Shen, C., et al., 2020. An accelerated active-set algorithm for a quadratic semidefinite program with general constraints. Computational Optimization and Applications, pp.1-42.

[44] Abide, S., et al., 2021. Inexact primal–dual active set method for solving elastodynamic frictional contact problems. Computers & Mathematics with Applications, 82, pp.36-59.

Submitted: 08.05.2021.

Revised: 16.08.2021

Accepted: 21.8.2021.